



LAWRENCE
LIVERMORE
NATIONAL
LABORATORY

Analysis Procedures for Double-Shell Target Concentricity and Wall Thickness

J. D. Sain, W. D. Brown, H. E. Martz, D. J.
Schneberk

March 28, 2006

Disclaimer

This document was prepared as an account of work sponsored by an agency of the United States Government. Neither the United States Government nor the University of California nor any of their employees, makes any warranty, express or implied, or assumes any legal liability or responsibility for the accuracy, completeness, or usefulness of any information, apparatus, product, or process disclosed, or represents that its use would not infringe privately owned rights. Reference herein to any specific commercial product, process, or service by trade name, trademark, manufacturer, or otherwise, does not necessarily constitute or imply its endorsement, recommendation, or favoring by the United States Government or the University of California. The views and opinions of authors expressed herein do not necessarily state or reflect those of the United States Government or the University of California, and shall not be used for advertising or product endorsement purposes.

This work was performed under the auspices of the U.S. Department of Energy by University of California, Lawrence Livermore National Laboratory under Contract W-7405-Eng-48.

Analysis Procedures for Double-Shell Target Concentricity and Wall Thickness ¹

John Sain, Bill Brown, Harry Martz, Dan Schneberk
Lawrence Livermore National Laboratory (LLNL), Livermore, CA

INTRODUCTION

The LLNL Target Fabrication Team (TFT) asked the Center for Non-Destructive Characterization (CNDC) to use CNDC's KCAT or Xradia's Micro computed tomography (CT) system to collect three-dimensional (3D) tomographic data of a set of double-shell targets and determine, among other items, the following: (1) the concentricity of the outer surface of the inner shell with respect to the inner surface of the outer shell with an accuracy of 1-2 micrometers, and (2) the wall thickness uniformity of the outer shell with an accuracy of 1-2 micrometers. The CNDC used Xradia's Micro CT system to collect the data. Bill Brown performed the concentricity analysis, and John Sain performed the wall thickness uniformity analysis. Harry Martz provided theoretical guidance, and Dan Schneberk contributed technical (software) support. This document outlines the analysis procedures used in each case.

The double-shell targets, as shown in Figures 1 and 2, consist of an inner shell (or capsule), a two-piece spherical aerogel intermediary shell, and a two-piece spherical outer shell². The three elements are designed and fabricated to be concentric – with the aerogel shell acting as a spacer between the inner shell and outer shell – with no to minimum air gaps in the final assembly. The outer diameters of the aerogel and outer shells are 444 and 550 micrometers, respectively, so the wall thickness of the outer shell is 53 micrometers.

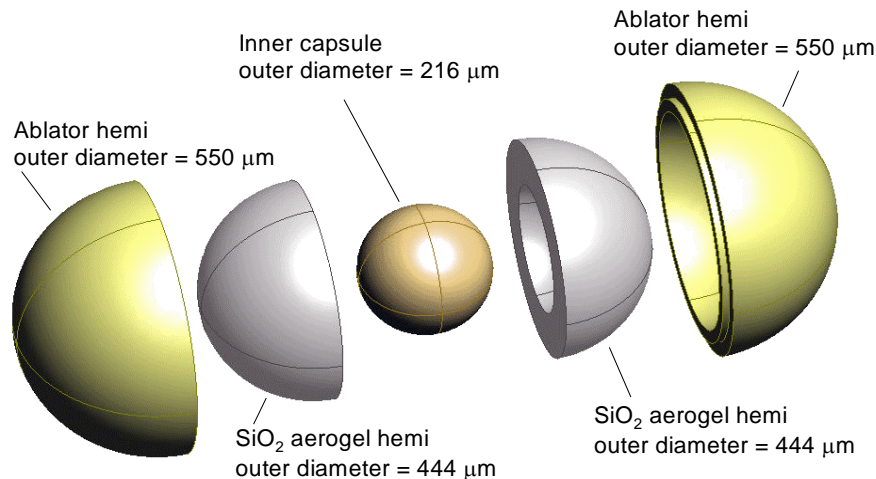


Figure 1. Schematic of the components that make up a double-shell target.

¹ This work was performed under the auspices of the U.S Department of Energy by the University of California, Lawrence Livermore National Laboratory under Contract No. W-7405-Eng-48.

² Figures 1 and 2 were taken from "Development of a Manufacturing Process for Double-Shell Targets", a Lawrence Livermore National Laboratory poster (UCRL-POST-209776) created by M. Bono, R. Hibbard, D. Bennett, *et al.*

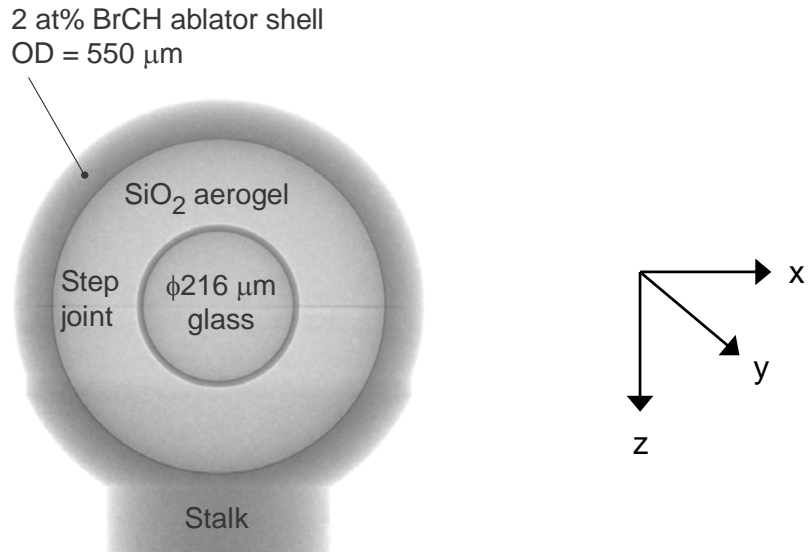


Figure 2. Digital radiograph of a double-shell target obtained using Xradia’s Micro CT system.

DATA ANALYSIS PROCEDURES

The data analysis procedures used to determine both the concentricity and wall thickness consist of a series of steps that were specifically developed for analysis of double-shell CT data sets. This section provides a step-by-step description of each procedure. The data analysis was performed on x-, y-, and z-sliced CT data. For reference purposes, the z-axis passes through the center of the glass inner shell and is collinear with the axis of the stalk (as shown in Figure 2). The concentricity and wall thickness uniformity analyses were performed using IDL software and CNDC’s “imgrec” image processing program (Dan Schneberk, originator), respectively.

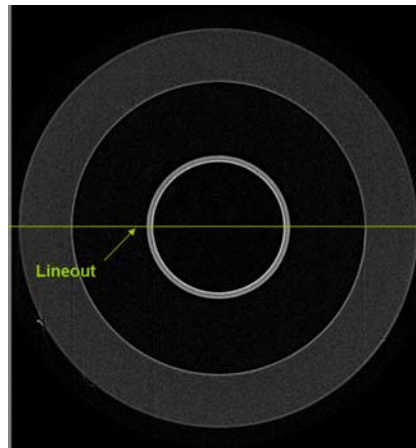
Concentricity of outer and inner shells

The procedure to calculate the concentricity of the outer and inner shells of a double-shell target requires several steps. For a specified orthogonal direction (x, y, or z) and shell (outer or inner), the essential approach, for each CT data slice, is to determine the two coordinates representing the physical center of each reconstructed shell. The initial step in the procedure is to assign a binary value (e.g. 0 or 1) to each voxel within the data slice. Voxels located within the region (e.g. shell) of interest will – ideally – be assigned a value of one while all other voxels within the data slice will be assigned a value of zero. Using this binary image, the remaining steps in the procedure are to perform a cluster analysis of the voxel values to isolate the voxels associated with the shell, execute a morphological dilation program to determine the region occupied by voxels inside the shell boundary of interest, and calculate the center of mass and volume of the bounded region. The center-of-mass coordinates, one set from each data slice, are used to generate a sample mean and standard deviation for the center-of-mass coordinates for all of the slices. Performing a similar analysis on the other shell will allow one to compare the estimated center-of-mass coordinates of the shell surfaces. Performing the

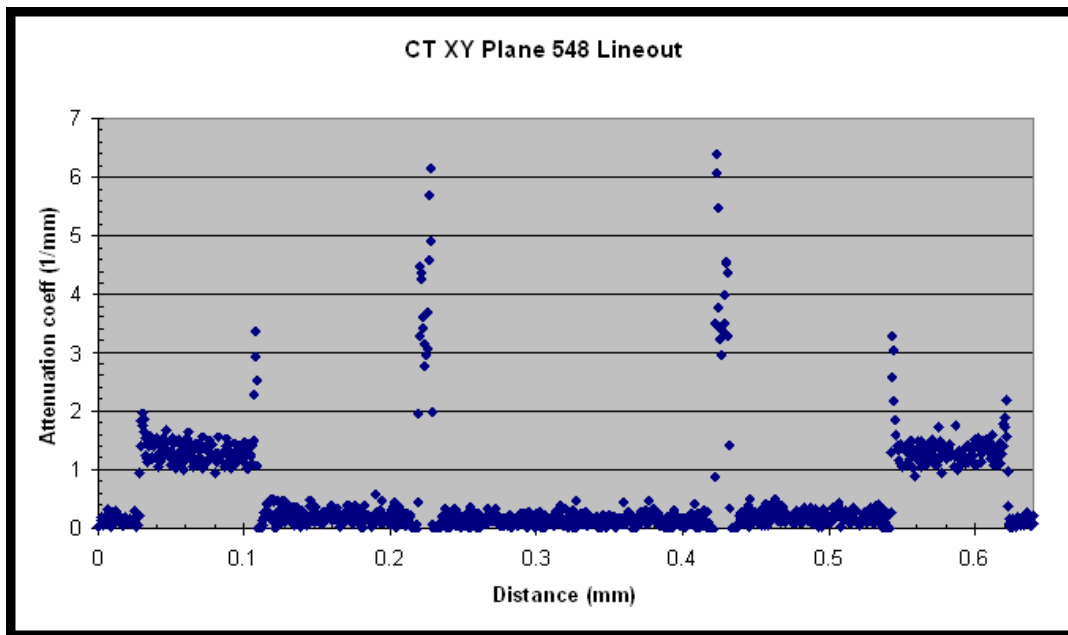
analysis for both shells in each of the other two orthogonal directions provides two more sets of sample means and standard deviations for each of the three coordinates (x, y, and z) – from which one can estimate the actual concentricity of the two shells.

Outer shell

To begin we create a "line-out" (Figure 3) that runs from the outside air (outside the outer shell) into the aerogel region between the outer and inner shells. A threshold level is determined by choosing an approximate midpoint value between the air and outer shell voxel values. In the sample case shown below, we selected a threshold of 1.0 mm^{-1} .



(a)



(b)

Figure 3. (a) CT data slice near center of double-shell target along z-axis. (b) Line out for the line shown in (a).

The binary image (Figure 4) is created using the threshold level of 1.0 by assigning a value of zero to voxels with values less than 1.0 and a value of one to voxels with values equal to or greater than 1.0.

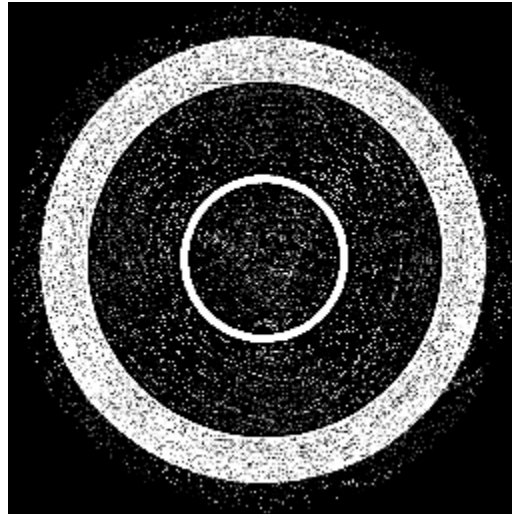


Figure 4. Binary image of the CT data slice shown in Figure 3(a).

Next we run a cluster analysis on the binary image data, and we sort the data clusters with respect to cluster volume. There can be as many as five large clusters created after sorting depending on which data slice that we are currently processing. All possible clusters shown in Figure 5 are listed in order of descending volume: (1) air outside the outer shell, (2) aerogel bounded by the outer and inner shells, (3) outer shell material (BrCH), (4) air inside the inner shell, and (5) inner shell material (SiO₂ glass).

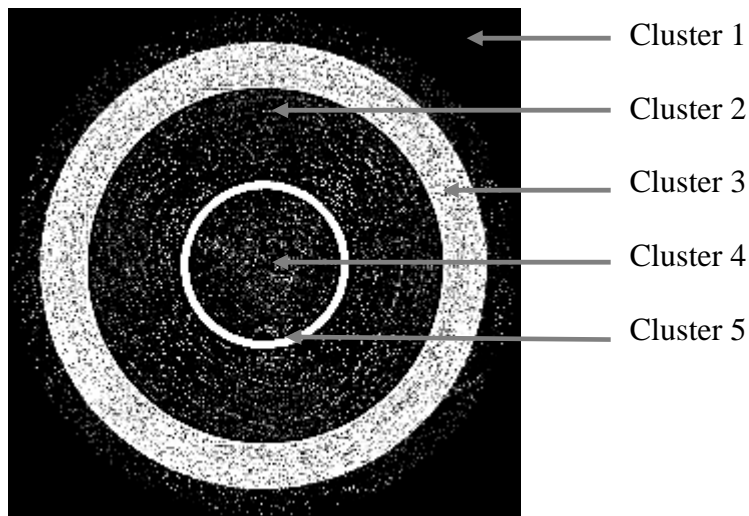


Figure 5. The five possible voxel clusters listed in order (from 1 to 5) of descending volume.

We set the values of all clusters to zero except for Cluster 3 (the cluster representing the outer shell), which is set to one. This produces an image (Figure 6) of all zeros except for the voxels representing the outer shell material.

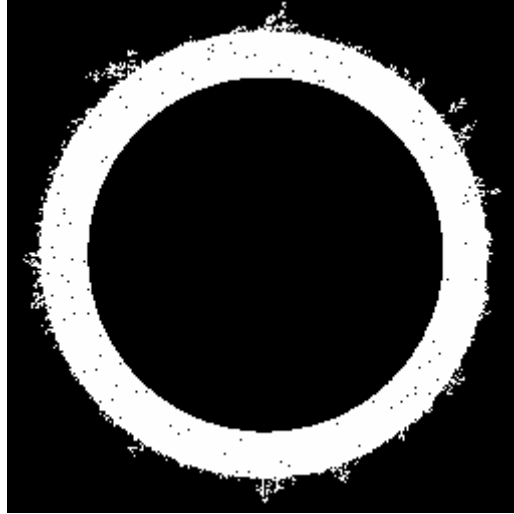


Figure 6. Cluster 3, representing the outer shell material, remains after the voxel values of the other clusters are set to zero.

Next we create a scratch image with the same dimensions as the CT data slice image. We assign a value of zero to all voxels in the scratch image except for the center voxel, which is assigned a value of one. Starting at the center voxel, we begin a “Do-Loop” that uses the morphological filter “Dilate” to grow the number of ones on the scratch image. After each pass through the “Do-Loop”, the scratch image is compared to the cluster image (Figure 6). If corresponding voxels in the scratch and cluster images (e.g. voxels occupying the same location in each image) both have values of one, then the value of the scratch image voxel is reassigned to zero. The group of voxels with a value of one within the scratch image continues to grow until it occupies the region of space bounded by Cluster 3. A sample sequence of dilations is shown in Figure 7.

Finally, we calculate (a) the xy coordinate pair that represents the center of mass for and (b) the actual physical volume represented by the set of voxels within the scratch image that have a value of one. The x and y coordinates for the center of mass are independently found using the equations

$$x_{cm} = \frac{\sum_i^N m_i x_i}{\sum_i^N m_i} = \frac{\sum_i^N x_i}{N} \qquad y_{cm} = \frac{\sum_i^N m_i y_i}{\sum_i^N m_i} = \frac{\sum_i^N y_i}{N}$$

for which $m_i = 1$ for all i and N is the number of voxels having a value of one. The actual physical volume represented by the set of voxels with a value of one is found by multiplying N by the actual physical volume of a voxel. All of this data is subsequently written to an Excel spreadsheet.

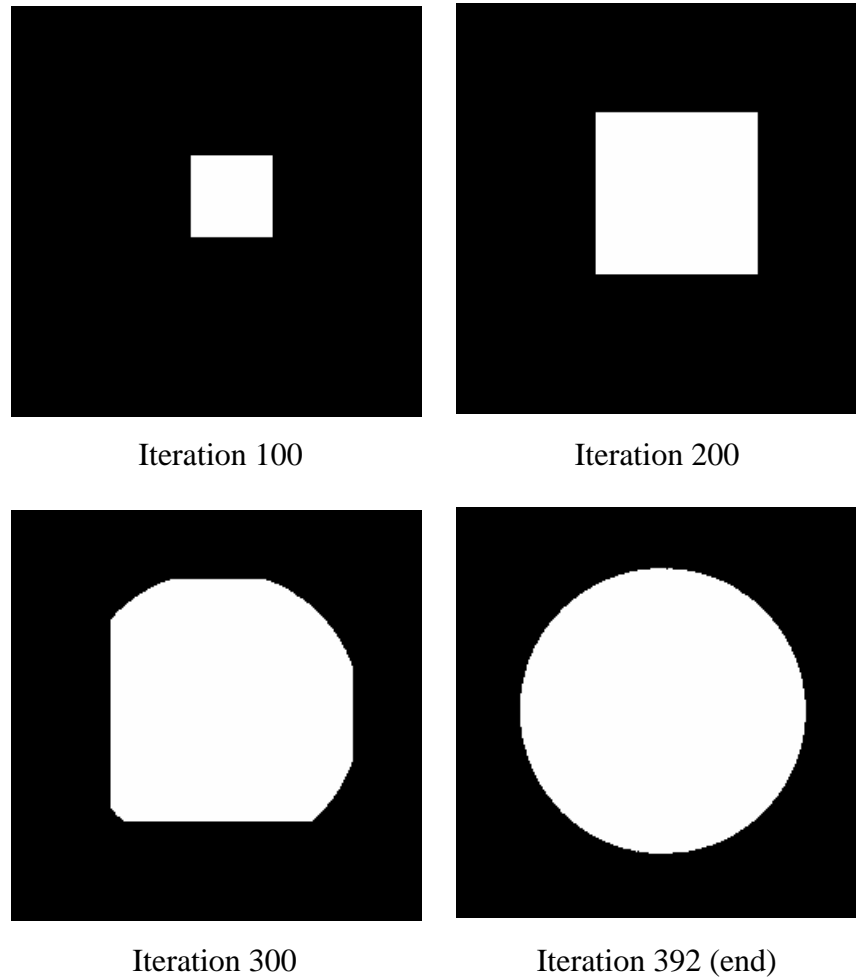


Figure 7. Sample sequence of images illustrating how the IDL morphological filter "Dilate" is used to determine the region of space bounded by Cluster 3.

Inner shell

The procedure for the inner shell is similar to that for the outer shell, but we work with the outer surface of the inner shell instead of the inner surface of the outer shell. We perform the same thresholding and cluster analysis as outlined above, but in this case we set the value of all clusters to zero except for Cluster 5 (the cluster representing the inner shell), which is set to one. Once again, we generate a scratch image consisting of all zeros except for the center pixel that has a value of one. Starting from the center pixel, the morphological filter "Dilate" is used to establish a contiguous set of voxels, each having a value of one, that completely fills the region bounded by Cluster 5. This leaves us with an image of zeros everywhere except for the region bounded by the outer surface of the inner shell. We calculate the center-of-mass coordinates and volume for the set of voxels having a value of one and then write this data to the Excel spreadsheet.

Wall thickness of outer shell

The procedure to find the wall thickness of the outer shell involves multiple steps. For each of the six targets and three orthogonal orientations, we estimate which data slice passes through the center of the target shells. Image-processing software is then used to remove all physical features of the double shell target except for the outer shell. The image voxels corresponding to the outer shell are filtered and binarized to remove extraneous voxel values. An analysis algorithm is then executed on the outer shell data to estimate the wall thickness at an extensive number of locations. Sample statistics for the wall thickness are formed and reported.

Central slice selection

Using the shell concentricity analysis data, the center slice, or the slice that is estimated to contain the largest volume inside the boundary defined by the inner surface of the outer shell, is determined for the x-slice, y-slice, and z-slice data of each target. Using CNDC's "imgrec" image processing program, the slice data is brought up for viewing and analysis. For example, z-slice 569 for Target 1 is shown in Figure 8 with the inner and outer shells and the aerogel labeled.

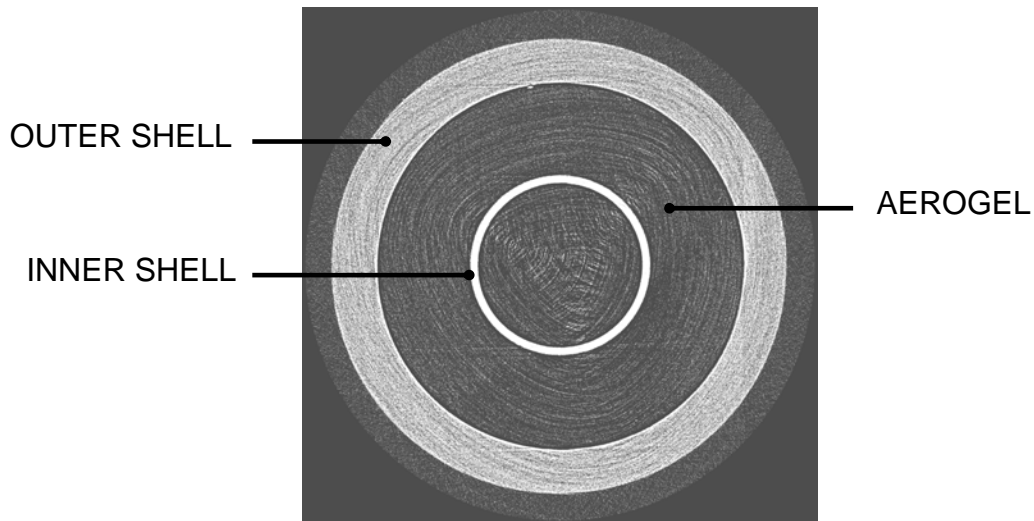


Figure 8. Sample image of CT slice data (Target 1, z-slice 569) containing a cross-section of the outer and inner shells and the aerogel between the shells.

Interior mask

Using the "Circle Sizing" tool in "imgrec", a circle (shown in red in Figure 9a) is placed just inside the boundary between the aerogel and inner surface of the outer shell. We record the center coordinates and the radius of the circle. Using the "Circ-Mask" tool (imgrec: "Transform" menu), the region inside the circle is masked off by setting the voxel values to zero (Figure 9b).

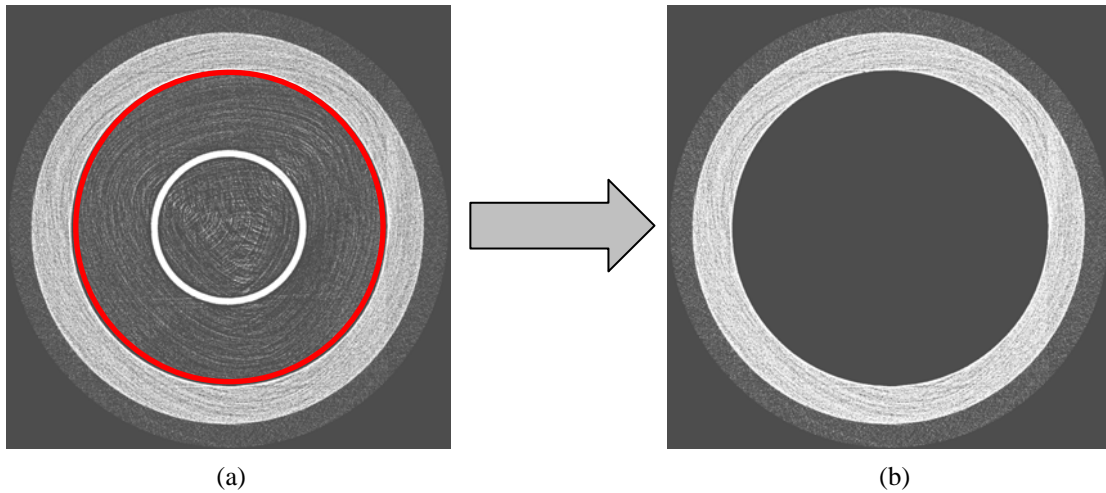


Figure 9. Pair of images depicting how we use the (a) “Circle Sizing” and (b) “Circ-Mask” tools in the “imgrec” software to mask off the voxels that are defined to be inside the inner surface of the outer shell.

Exterior Mask

Using the Circle Sizing tool again, a circle (shown in red in Figure 10a) is placed just outside the outer surface of the outer shell. We again record the center coordinates and radius of the circle. Using the Circ-Mask tool, the region outside the circle is masked off by setting the voxel values to zero (Figure 10b).

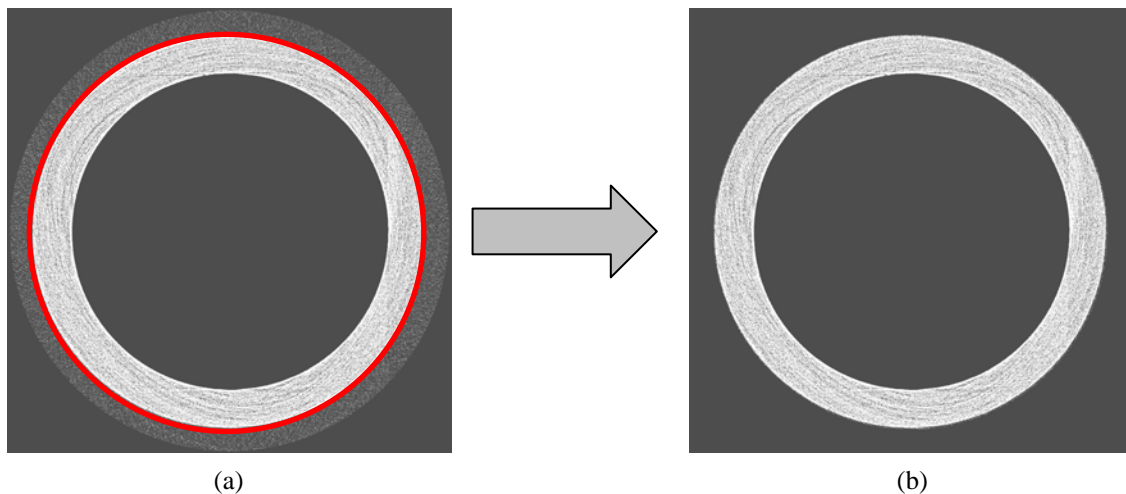


Figure 10. Pair of images depicting how we use the (a) “Circle Sizing” and (b) “Circ-Mask” tools in the “imgrec” software to mask off the voxels that are defined to be outside the outer surface of the outer shell.

Median filter and binarization

Using the “Median” tool (imgrec: Transform menu), a median filter (5 x 5 voxel kernel) is applied to the remaining data to reduce the fluctuations in the voxel values while preserving critical edge gradients. Using the “Make-Binary” tool (imgrec: Transform menu), a binary filter with an appropriate threshold is applied in an effort to

set to zero any remaining voxels that are located outside the boundaries of the outer shell (Figure 11b).

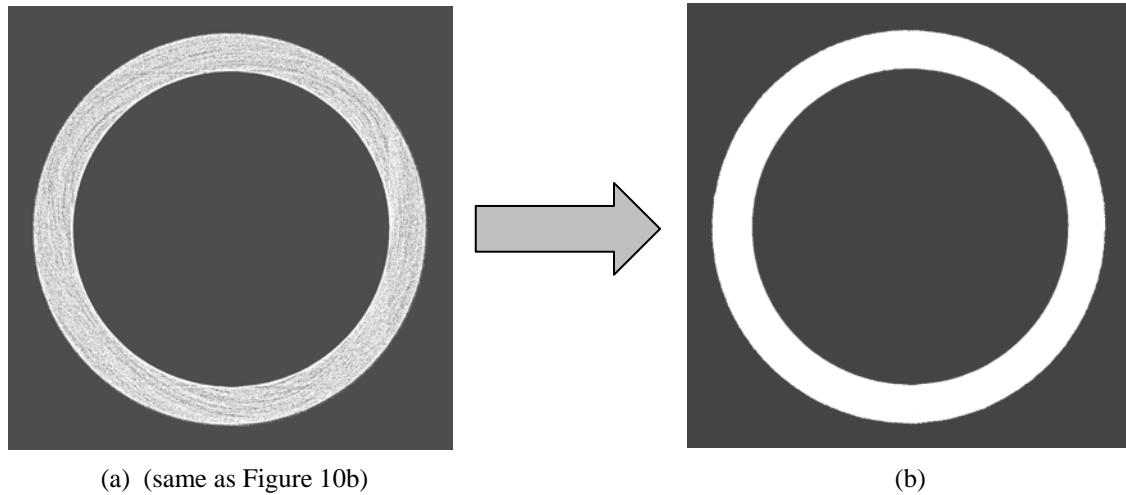


Figure 11. Pair of images depicting how we use the “Median” and “Make-Binary” tools in the “imgrec” software to filter and binarize the image data in order to remove extraneous (e.g. outlying) voxel values.

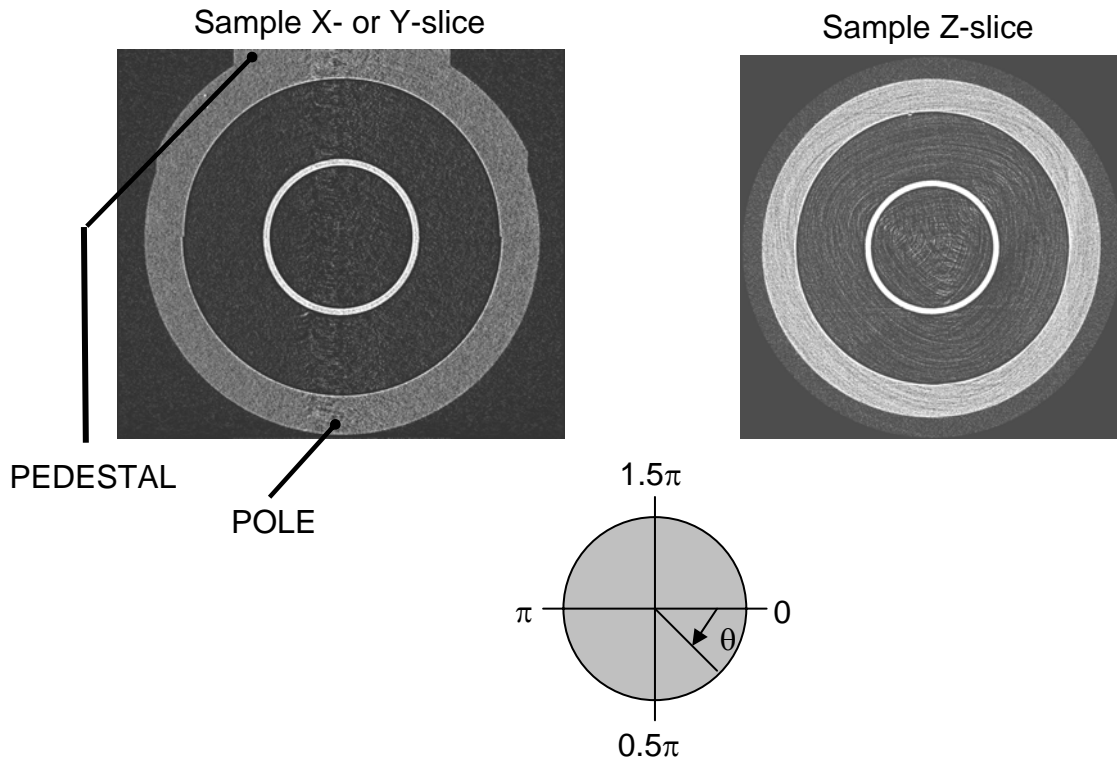


Figure 12. Sample orthogonal images of CT slice data. The image on the left represents slice data in an xz or yz plane. (Note that the image is flipped relative to that shown in Figure 2.) The image on the right depicts slice data in a xy plane. The pedestal and pole of the double-shell target are labeled for reference. Note that any angular ranges are defined such that the magnitude of the angle increases in the clockwise direction.

Wall thickness calculation

Using the “Get-Wall-CircFit” or “Get-W-Circ-User” tool (imgrec: “ImageCalc” menu), we calculate sample estimates of the outer shell wall thickness. For the x- and y-slice data, the wall thickness is estimated at over 650 angular locations over a 170-degree range (from 5° to 175° in the clockwise direction; see Figure 12) on the top half (the half not attached to the pedestal) of the shell. For the z-slice data, the wall thickness is estimated at over 1400 angular locations over a 360-degree range. The statistical wall thickness values reported include the mean, standard deviation, maximum, and minimum.

For the x- and y-slice data, sample estimates of the wall thickness of the outer shell at the pole, the point on the shell located directly opposite – and furthest – from the center of the pedestal (or stalk), were also calculated. The wall thickness estimates were obtained from eight angular locations evenly spaced over a range of two degrees centered upon the pole.

RESULTS

Concentricity of outer and inner shells

The results of the concentricity analysis are summarized in Table 1. The mean x-, y-, and z-coordinates for the center of each of the six targets are listed by row. The appropriate comparison to make is to compare the mean coordinate – in a specified axial direction – for the outer shell with that of the inner shell. For example, for Target 6 the mean center coordinates are $(x, y, z) = (512.45, 380.18, 511.26)$ for the outer shell and $(x, y, z) = (511.79, 379.17, 513.32)$ for the inner shell. The magnitudes of the differences, or $(|\Delta x|, |\Delta y|, |\Delta z|) = (0.66, 1.01, 2.06)$ in units of voxels, demonstrate that the estimated centers of the inner and outer shells are located only 2.39 voxels, or 1.46 micrometers, apart. The last column of the table indicates that the distance between the shell center locations ranges from 0.53 to 1.68 micrometers. The mean center separation for all six

Table 1. Summary of the mean voxel dimensions, mean center coordinates for the outer and inner shells, and the rms distance between the estimated center locations for six different double-shell targets.

Target number	Mean voxel size (μm)	Mean coordinate (voxel number)						RMS vector length (voxels)	RMS vector length (μm)
		Outer shell			Inner shell				
		x	y	z	x	y	z		
1	0.612	512.90	432.23	513.75	511.78	432.54	511.88	2.21	1.35
2	0.591	514.25	396.90	511.56	512.32	395.85	513.13	2.69	1.59
3	0.612	514.32	385.29	512.67	511.66	385.96	512.48	2.75	1.68
6	0.612	512.45	380.18	511.26	511.79	379.17	513.32	2.39	1.46
7	0.612	546.68	412.36	549.67	549.30	412.77	550.16	2.70	1.65
8	0.612	512.70	393.25	512.53	511.84	393.14	512.41	0.87	0.53

targets is 1.38 ± 0.40 micrometers. If the 0.53-micrometer data value for Target 8 is excluded – simply because its magnitude is much less than that of the other data values, then the mean center separation for the remaining five targets is 1.55 ± 0.21 micrometers.

The double-shell target design specifications called for concentric shells, or, ideally, that $(|\Delta x|, |\Delta y|, |\Delta z|) = (0, 0, 0)$, and the CNDC was asked to measure the actual distance between the shell center locations to an accuracy of 1-2 micrometers. The reader should remember as well that the center coordinates of the inner and outer shells are derived from their outer and inner surfaces, respectively.

Wall thickness of outer shell

The mean, standard deviation, maximum, and minimum wall thickness values for the outer shell of each target are tabulated in Tables 2-4 for each data slice orientation. The wall thickness sample statistics for the x- and y-slice data, shown in Tables 2 and 3, are split into two categories: “global” and “pole”. The “global” statistics are derived from over 650 wall thickness sample values over an angular range of $[5^\circ, 175^\circ]$ in which, as illustrated in Figure 12, angle values increase in the clockwise direction. The angular range, chosen by the CNDC, provides a large number of sample wall thickness values from a region of the shell that is not attached to the pedestal. The “pole” statistics are derived from eight wall thickness sample values over an angular range of $[89^\circ, 91^\circ]$, a 2° range, specified by the TFT, that is centered upon the pole of the target shells. The wall thickness sample statistics for the z-slice data, shown in Table 4, are in the “global” category. In this case, since the pedestal structure is not present in the data slice image under analysis, the statistics are derived from over 1400 wall thickness values over the complete angular range of $[0^\circ, 360^\circ]$. The wall thickness sample statistics for each target shell, presented in Table 5, are derived by combining, with an appropriate statistical method, the sample statistics for each target shell from the x-, y-, and z-slice data in Tables 2-4. The mean wall thickness for all six targets is 51.01 ± 1.02 micrometers. If the 54.47 ± 0.79 -micrometer data value for Target 7 is excluded – simply because its magnitude is much greater than that of the other data values, then the mean wall thickness for the remaining five targets is 50.31 ± 1.06 micrometers.

The double-shell target design specifications called for an outer shell wall thickness of 53 micrometers, and the CNDC was asked to measure the actual wall thickness to an accuracy of 1-2 micrometers. The CNDC analysis satisfies the request for 1-2 micrometer accuracy, but the reported sample statistical values for wall thicknesses do not satisfy the 53-micrometer design specification. The mean wall thickness of 50.31 ± 1.06 micrometers for Targets 1, 2, 3, 6, and 8 is less than 53 micrometers, and wall thickness of 54.47 ± 0.79 micrometers for Target 7 is greater than 53 micrometers.

The raw wall thickness data can detect very subtle manufacturing defects in the target shells. The introduction to Appendix A describes how an anomalous dip in the wall thickness values for some Target 6 z-slice data led to the discovery that the outer surface of the outer shell is slightly flattened in a local area. The defect is clearly seen in an accompanying image (Figure 13). For reference, Appendix A contains a complete set of plots – one for each combination of data slice orientation and target number – that illustrate the outer shell wall thickness results upon which this analysis is based.

Table 2. Summary of sample statistics for the wall thickness of the outer shell of each target as determined from the x-slice data.

TARGET	GLOBAL ¹ [5°, 175°]				POLE ² [89°, 91°]	
	MEAN [μm]	STD DEV [μm]	MAX [μm]	MIN [μm]	MEAN [μm]	STD DEV ³ [μm]
1	51.14	0.47	52.20	49.52	51.22	0.00
2	49.59	0.35	50.44	48.46	49.73	0.25
3	51.56	0.61	52.52	49.68	51.52	0.28
6	50.37	0.46	51.63	48.95	49.94	0.18
7	54.39	0.46	55.86	53.24	53.86	0.00
8	49.92	0.53	51.22	48.38	50.07	0.06

¹ Statistics calculated from over 650 wall thickness sample values over an angular range of [5°, 175°].

² Statistics calculated from 8 wall thickness sample values over an angular range of [89°, 91°], a 2° range centered upon the "pole" of the target shells.

³ A standard deviation of zero simply indicates that all 8 samples were equal.

Table 3. Summary of sample statistics for the wall thickness of the outer shell of each target as determined from the y-slice data.

TARGET	GLOBAL ¹ [5°, 175°]				POLE ² [89°, 91°]	
	MEAN [μm]	STD DEV [μm]	MAX [μm]	MIN [μm]	MEAN [μm]	STD DEV ³ [μm]
1	50.96	1.52	53.34	47.24	51.22	0.00
2	49.75	0.34	50.44	48.46	49.91	0.00
3	51.37	0.93	52.77	48.95	51.65	0.23
6	50.21	0.46	51.22	48.70	49.89	0.28
7	54.49	0.56	55.86	52.80	54.17	0.26
8	49.77	0.39	50.66	48.54	49.73	0.26

¹ Statistics calculated from over 650 wall thickness sample values over an angular range of [5°, 175°].

² Statistics calculated from 8 wall thickness sample values over an angular range of [89°, 91°], a 2° range centered upon the "pole" of the target shells.

³ A standard deviation of zero simply indicates that all 8 samples were equal.

Table 4. Summary of sample statistics for the wall thickness of the outer shell of each target as determined from the z-slice data.

TARGET	GLOBAL ¹ [0°, 360°]			
	MEAN [μm]	STD DEV [μm]	MAX [μm]	MIN [μm]
1	50.11	1.44	52.93	47.40
2	49.03	0.32	49.91	48.08
3	50.40	0.88	52.20	48.54
6	49.43	0.52	50.66	46.99
7	54.62	0.69	56.08	52.37
8	49.39	0.51	50.66	47.97

¹ Statistics calculated from over 1400 wall thickness sample values over an angular range of [0°, 360°].

Table 5. Summary of sample statistics for the wall thickness of the outer shell of each target as determined by combining the sample statistics from the x-, y-, and z-slice data presented in Tables 2-4.

TARGET	COMBINED			
	MEAN [μm]	STD DEV [μm]	MAX [μm]	MIN [μm]
1	50.87	1.73	53.34	47.24
2	49.55	0.51	50.44	48.08
3	51.26	1.18	52.77	48.54
6	50.13	0.69	51.63	46.99
7	54.47	0.79	56.08	52.37
8	49.76	0.70	51.22	47.97

SUMMARY

At the request of the LLNL Target Fabrication Team, the LLNL Center for Non-Destructive Characterization used Xradia's Micro CT system to collect 3D tomographic data of a set of double-shell targets in order to determine, among other items, the (1) concentricity of the outer surface of the inner shell with respect to the inner surface of the outer shell with an accuracy of 1-2 micrometers and (2) wall thickness uniformity of the outer shell with an accuracy of 1-2 micrometers. The double-shell target design specifications called for (1) concentric shells and (2) an outer shell wall thickness of 53 micrometers.

With respect to shell concentricity, the physical locations of the shell centers for all but one target (Target 8) have a mean separation of 1.55 ± 0.21 micrometers. Specifically, the calculated distances between the center locations of Targets 1, 2, 3, 6, 7, and 8 are 1.35, 1.59, 1.68, 1.46, 1.65, and 0.53 micrometers, respectively, as shown in Table 1. The mean center separation for all six targets is 1.38 ± 0.40 micrometers. If the 0.53-micrometer data value for Target 8 is excluded from the calculation – simply because its magnitude is much less than that of the other data values, then the mean center separation for the remaining five targets is 1.55 ± 0.21 micrometers.

With respect to wall thickness uniformity, the outer shell wall for all but one target (Target 7) has a mean thickness of 50.31 ± 1.06 micrometers – nearly 3 micrometers less than the 53-micrometer specification. Specifically, the calculated outer-shell wall thicknesses of Targets 1, 2, 3, 6, 7, and 8 are 50.87 ± 1.73 , 49.55 ± 0.51 , 51.26 ± 1.18 , 50.13 ± 0.69 , 54.47 ± 0.79 , and 49.76 ± 0.70 micrometers, respectively, as shown in Table 5. The mean wall thickness for all six targets is 51.01 ± 1.02 micrometers. If the 54.47 ± 0.79 -micrometer data value for Target 7 is excluded from the calculation – simply because its magnitude is much greater than that of the other data values, then the mean wall thickness for the remaining five targets is 50.31 ± 1.06 micrometers.

Also with respect to wall thickness uniformity, the raw wall thickness data is capable of depicting very subtle manufacturing defects in the target shells. For example, as described and illustrated in Appendix A, an anomalous dip in the wall thickness values for Target 6 indicated the presence of a slightly flattened region on the outer surface of its outer – and ideally spherical – shell.

Appendix A. Data for wall thickness as a function of angle.

This appendix contains eighteen plots of wall thickness data as a function of angle. The plots represent each combination of data slice orientation (x, y, z) and double shell target number (1, 2, 3, 6, 7, 8). The first set of six plots is the x-slice data, the second set of six plots the y-slice data, and the third set of six plots the z-slice data. For reference, Figure 12 contains samples of the x-, y-, and z-slice data. Note that the pedestal, or the base (or stalk) of the target fixture, appears in the x- and y-slice data, and so the wall thickness is estimated only for a 170-degree range – from 5 to 175 degrees in the clockwise direction (See Figure 12 above.). On the other hand, the pedestal does not appear in the z-slice data, and so the wall thickness is estimated for the full 360-degree range. Note that the angles progress from 0 to 360 degrees in a clockwise direction.

The raw wall thickness data can illustrate subtle manufacturing defects in the double-shell targets. For example, an anomaly in the wall thickness data values is observed near the angle of 4.3 radians in the plot for z-slice 426 of Target 6. A visual inspection of the image for the z-slice 426 data, shown in Figure 13, determines that the anomalous data values correspond to a slightly flattened region of the outer surface of the outer shell. This region is indicated by the red rectangle in Figure 13. The wall thickness in this region is about 2 micrometers less than that in other areas.

Figure 13. Image of z-slice 426 data from Target 6. The red rectangle indicates a slightly flattened region of the outer surface of the outer shell.

